Extracting elements of molecular structure from the all-particle wave function

AIP | The Journal of Chemical Physics

Extracting elements of molecular structure from the all-particle wave function

Edit Mátyus, Jürg Hutter, Ulrich Müller-Herold, and Markus Reiher

Citation: J. Chem. Phys. **135**, 204302 (2011); doi: 10.1063/1.3662487
View online: http://dx.doi.org/10.1063/1.3662487
View Table of Contents: http://jcp.aip.org/resource/1/JCPSA6/v135/i20
Published by the American Institute of Physics.

Extracting elements of molecular structure from the all-particle wave function

Edit Mátyus,[1,a)] Jürg Hutter,[2] Ulrich Müller-Herold,[3] and Markus Reiher[1]
[1]*Laboratory of Physical Chemistry, ETH Zürich, Wolfgang-Pauli-Str. 10, CH-8093 Zürich, Switzerland*
[2]*Institute of Physical Chemistry, University of Zürich, Winterthurerstrasse 190, CH-8057 Zürich, Switzerland*
[3]*Institute of Biogeochemistry and Pollutant Dynamics, ETH Zürich, Universitätstrasse 16, CH-8092 Zürich, Switzerland*

(Received 17 June 2011; accepted 1 November 2011; published online 23 November 2011)

Structural information is extracted from the all-particle (non-Born–Oppenheimer) wave function by calculating radial and angular densities derived from *n*-particle densities. As a result, one- and two-dimensional motifs of classical molecular structure can be recognized in quantum mechanics. Numerical examples are presented for three- (H^-, Ps^-, H_2^+), four- (Ps_2, H_2), and five-particle (H_2D^+) systems. © *2011 American Institute of Physics*. [doi:10.1063/1.3662487]

I. INTRODUCTION

The conceptual basis of chemistry has been developed as a complex interplay of experiments, models, and so-called "paper tools" during the last two centuries.[1,2] As a result, the core terminology of chemistry now includes the notions *atom, molecule, chemical composition, molecular structure, isomer, conformer, chirality, enantiomer, bond, valence, and connectivity.* Although these notions were often not defined with formal terms, they are central to classical chemical thinking and were used in designing new materials and inventing new reaction pathways.

In the first part of the 20th century the success of quantum mechanics in the quantitative description of various physical and spectroscopic experiments suggested that it may serve as a fundamental mathematical theory for low-energy physics, including the molecular domain. Indeed, following the pioneering work of Heitler and London[3] relying on the Born–Oppenheimer (BO) separation[4] of electrons and nuclei quantum mechanics was adapted for chemical systems and the field of electronic structure theory has been launched. Computer programs were developed during the last five decades for the numerical solution of the electronic Schrödinger equation with clamped nuclei and serve nowadays as practical tools in explaining and predicting a large number of physical and chemical properties of molecular systems.[5]

However, since classical chemistry and quantum mechanics developed independently there is a natural semantic barrier constricting the translation of genuine chemical notions into the formalism of quantum mechanics. One example—the one to which the present work is devoted—is the concept of molecular structure in quantum mechanics.

At the elementary physical level molecules are assemblies of electrons and nuclei associated with some mass, electric charge, and spin. Thus, by solving the all-particle Schrödinger equation, non-relativistic energies and wave functions can be obtained. At present it is not clear, however, how the molecular structure and the related concepts of molecular symmetry, isomerism, and chirality can be reconstructed from the solutions of the all-particle Schrödinger equations.[6–14]

In the current practice of quantum chemistry and electronic structure theory the BO or clamped nuclei approximation[4,15,16] is almost always introduced. In the first step it allows one to simplify the all-particle problem to a quantum mechanical problem of electrons moving in the external field of fixed, classical, distinguishable nuclei. Within this framework the equilibrium structure is defined as the arrangement of nuclei which minimizes the sum of the electronic and the classical nuclear-nuclear repulsion energies. This definition of molecular structure or the even more sophisticated effective rovibrationally and thermally averaged variants[17,18] are based on the introduction of the BO separation and thus assume the existence of a certain structure.[19–21]

Mathematically, Primas characterized the BO electronic Schrödinger equation in the 1980s as an asymptotic singular limit of the all-particle case.[19,22] In various fields of physics singular limits result in the emergence of qualitatively new properties for the theory.[23] According to Primas the emerging property in the BO singular limit would be the molecular structure.[19,22] It is desirable to clarify whether, at least elements of, the classical molecular structure can be recognized in the quantum theory without invoking additional assumptions or limiting considerations.

In a critical account Woolley[6] stated that "Quantum chemistry, however, has not as yet achieved this result, and instead the notion of molecular structure remains a stark mystery which [. . .] is simply said to be demanded by the known facts." The problem of the notion of molecular structure in quantum mechanics was explicitly formulated[6] and explained which also underlined the differences between BO electronic structure and all-particle calculations. Such an important difference is that the all-particle Hamiltonian describes not only the electrons but also the identical nuclei as indistinguishable quantum particles. Then, by calculating the expectation value for the distance of a nucleus picked out from the set of type *X* and another one from the set of type *Y* nuclei, a single mean value is obtained even if in the classical molecular structure

a)Electronic mail: edit.matyus@phys.chem.ethz.ch.

one would measure several different X–Y bond lengths.[11,13,24] This problem was described in a numerical all-particle study of the H_3^+ molecular ion by Cafiero and Adamowicz.[12] By calculating the expectation values of the proton-proton distance and the angle for the three protons it was not possible to decide whether the molecule has a linear or a triangular shape.

At the computational level, several algorithms and computer programs have been developed during the last two decades for the variational solution of the all-particle electron-nuclear Schrödinger equation following the pioneering work of Kołos and Wolniewicz[25] on the H_2 molecule. Suzuki and Varga developed the stochastic variational method in combination with Gaussian geminals.[26] Adamowicz and co-workers developed a variational method using Gaussian geminals in which the basis function coefficients were optimized by means of gradient techniques using analytic gradients.[27] Nakai,[28] Hammes-Schiffer and co-workers,[29,30] and Nagashima and co-workers[31] developed nuclear-electron orbital methods as an extension of molecular orbital methods of electronic structure theory. We may refer the reader to Sherrill and co-workers who presented a thorough and critical overview of nuclear-electronic orbital procedures.[32]

Besides the intellectual challenge of developing a numerical procedure for the solution of the all-particle Schrödinger equation, these investigations either provided exceedingly accurate non-relativistic energy levels and beyond[33] or contributed to a better understanding of hydrogen and proton tunneling in biochemical systems where it could be anticipated that the BO approximation fails.[34]

In the present work, small molecular systems are considered within non-relativistic all-particle quantum mechanics by means of a variational procedure joining the direction pioneered by Suzuki and Varga[26] and Adamowicz and co-workers.[12] After presenting the essential details of the numerical protocol, the evaluation of probability densities of structural parameters, related to n-particle densities, is discussed. The usefulness of these functions is presented through numerical examples and one- and two-dimensional motifs of the classical molecular structure are extracted from the ground-state all-particle wave functions of the three-particle H^-, Ps^-, and H_2^+, the four-particle Ps_2 and H_2, and the five-particle H_2D^+ molecular ion.

II. VARIATIONAL SOLUTION OF THE SCHRÖDINGER EQUATION OF MOLECULAR SYSTEMS WITHOUT CLAMPING THE NUCLEI

In this section we review the essential theory required to describe and analyze our calculations.

A. Coordinates and the Coulomb Hamiltonian

The Coulomb Hamiltonian for $N+1$ particles associated with masses m_i and electric charges q_i ($i = 1, 2, \ldots, N+1$) is

$$\hat{H}' = -\sum_{i=1}^{N+1} \frac{1}{2m_i} \Delta_{\boldsymbol{x}_i} + \sum_{i=1}^{N+1} \sum_{j>i}^{N+1} \frac{q_i q_j}{|\boldsymbol{x}_i - \boldsymbol{x}_j|} \tag{1}$$

in Hartree atomic units. Translational invariance is exploited by introducing the linear transformation of the coordinates $\boldsymbol{x}^{\mathrm{T}} = (\boldsymbol{x}_1, \boldsymbol{x}_2, \ldots, \boldsymbol{x}_{N+1})$ as

$$(\boldsymbol{r}_1, \boldsymbol{r}_2, \ldots, \boldsymbol{r}_n, \boldsymbol{x}_0)^{\mathrm{T}} = (\boldsymbol{U} \otimes \boldsymbol{I}_3)\boldsymbol{x} \in \mathbb{R}^{(N+1)\times 3}, \tag{2}$$

where $\boldsymbol{I}_3$ is the 3×3 unit matrix and the translational invariance of the coordinates $\boldsymbol{r}^{\mathrm{T}} = (\boldsymbol{r}_1, \boldsymbol{r}_2, \ldots, \boldsymbol{r}_N)$ imposes the following conditions on the elements of the constant $\boldsymbol{U} \in \mathbb{R}^{(N+1)\times(N+1)}$ matrix:

$$\sum_{j=1}^{N+1} U_{ij} = 0, \quad i = 1, 2, \ldots, N, \quad U_{N+1,j} = \frac{m_j}{m_{1\ldots N+1}}, \quad j = 1, 2, \ldots, N+1 \tag{3}$$

and $m_{1\ldots N+1} = \sum_{i=1}^{N+1} m_i$.[35,36] $\boldsymbol{x}_0$ denotes the coordinates of the center of mass (CM). The coordinates used in a calculation are defined by specifying the elements of $\boldsymbol{U}$, which fulfill the conditions of Eq. (3). In the present work Jacobi (Jac),

$$\boldsymbol{r}_i^{\mathrm{Jac}} = \sum_{j=1}^{i} \frac{m_j}{m_{1\ldots i}} \boldsymbol{x}_j - \boldsymbol{x}_{i+1}, \tag{4}$$

heavy-particle centered (HPC),

$$\boldsymbol{r}_i^{\mathrm{HPC}} = \boldsymbol{x}_i - \boldsymbol{x}_{N+1}, \tag{5}$$

and center-of-mass centered (CMC)

$$\boldsymbol{r}_i^{\mathrm{CMC}} = \boldsymbol{x}_i - \sum_{j=1}^{N+1} \frac{m_j}{m_{1\ldots N+1}} \boldsymbol{x}_j, \tag{6}$$

translationally invariant coordinates were used with $i = 1, 2, \ldots, N$, $m_{1\ldots i} = \sum_{j=1}^{i} m_j$, and the corresponding $\boldsymbol{U}$ matrices can be easily constructed.

Then, by expressing the quantum Hamiltonian in terms of the coordinates defined in Eq. (2) and after subtracting the kinetic energy of the center of mass, the translationally invariant Hamiltonian is obtained as

$$\hat{H} = -\sum_{k=1}^{N} \sum_{l=1}^{N} M_{kl} \nabla_{\boldsymbol{r}_k}^{\mathrm{T}} \nabla_{\boldsymbol{r}_l} + \sum_{k=1}^{N+1} \sum_{l>k}^{N+1} \frac{q_k q_l}{|\boldsymbol{f}_{kl}^{\mathrm{T}} \boldsymbol{r}|}, \tag{7}$$

where

$$M_{kl} = \sum_{i=1}^{N+1} \frac{U_{ki} U_{li}}{2m_i}, \quad k, l = 1, 2, \ldots, N \tag{8}$$

and

$$\boldsymbol{f}_{kl}^{\mathrm{T}} \boldsymbol{r} = \sum_{i=1}^{N} (\boldsymbol{f}_{kl})_i \boldsymbol{r}_i \tag{9}$$

with

$$(\boldsymbol{f}_{kl})_i = (\boldsymbol{U}^{-1})_{ki} - (\boldsymbol{U}^{-1})_{li}. \tag{10}$$

As the transformation from one set of translationally invariant coordinates to another is simple (linear) and the mathematical form of the basis functions (see Sec. II B) remains unchanged under linear transformations of the coordinates, always that set of coordinates was used which provided the technically most straightforward evaluation of integrals for

the kinetic and the potential energy matrix elements or particle densities.

B. Basis functions

Eigenfunctions of $\hat{H}$ are expressed as a linear combination of basis functions constructed as (anti)symmetrized products of spatial and spin functions:

$$\Phi_{SM_S}(\boldsymbol{r},\boldsymbol{\sigma}) = \hat{\mathcal{A}}\{\phi(\boldsymbol{r};\boldsymbol{C})\chi_{SM_S}(\boldsymbol{\sigma};\boldsymbol{\theta})\}, \tag{11}$$

where $\hat{\mathcal{A}} = (N_{\text{perm}})^{-1/2}\sum_{p=1}^{N_{\text{perm}}}\varepsilon_p\hat{\mathcal{P}}_p$ is the (anti)symmetrization operator. $\hat{\mathcal{P}}_p$ denotes possible permutations of identical particles and $\varepsilon_p = -1$ if $\hat{\mathcal{P}}_p$ represents an odd number of pair-interchange of fermionic coordinates, otherwise $\varepsilon_p = +1$. N_{perm} is the number of possible permutations of identical particles.

The spin part of the basis functions is constructed as[26,37]

$$\chi_{SM_S}(\boldsymbol{\sigma};\boldsymbol{\theta}) = \sum_{n=1}^{n_s}\lambda_n(\boldsymbol{\theta})\sigma_{M_S,n}, \tag{12}$$

where the primitive spin functions $\sigma_{M_S,n}$ are eigenfunctions of $\hat{S}_z$ with eigenvalue M_S and χ_{SM_S} is an eigenfunction of both $\hat{S}^2$ and $\hat{S}_z$. $\boldsymbol{\theta}$ contains real parameters to be optimized in the variational procedure, if the space corresponding to the same eigenvalues of $\hat{S}^2$ and $\hat{S}_z$ is larger than one-dimensional.

Eigenfunctions of the Hamiltonian are also angular momentum and parity eigenfunctions. Thus, it is convenient to use spatial basis functions that are angular momentum and parity eigenfunctions with the required eigenvalues. In the present work eigenstates corresponding to $L = 0$ angular momentum and $p = +1$ parity are studied, and thus a simple choice of the spatial functions can be Gaussian geminals[38]

$$\begin{aligned}\phi(\boldsymbol{r};\boldsymbol{C}) &= \exp[-\boldsymbol{r}^{\mathrm{T}}(\boldsymbol{C}\otimes\boldsymbol{I}_3)\boldsymbol{r}]\\ &= \exp\left[-\sum_{i=1}^{N+1}\sum_{j>i}^{N+1}a_{ij}(\boldsymbol{x}_i-\boldsymbol{x}_j)^2\right]\end{aligned} \tag{13}$$

with

$$A_{ij} = \delta_{ij}\left(\sum_{k=1,k\neq i}^{N+1}a_{ik}\right) + (1-\delta_{ij})(-a_{ij}) + c\,\frac{m_i m_j}{(m_{1\ldots N+1})^2}\,, \tag{14}$$

$i,j = 1,2,\ldots,N+1$, $c\in\mathbb{R}$, and

$$\begin{pmatrix}\boldsymbol{C} & \boldsymbol{0}\\ \boldsymbol{0} & c\end{pmatrix} = \boldsymbol{U}^{\mathrm{T}}\boldsymbol{A}\boldsymbol{U}\,. \tag{15}$$

Positive definiteness of $\boldsymbol{C}\in\mathbb{R}^{N\times N}$ guarantees that ϕ can be normalized on $\mathbb{R}^{N\times 3}$. Although this type of functions explicitly account for the particle-particle correlation, if rigorous convergence of the energy levels and wave functions was required, a computationally more efficient choice would be the inclusion of polynomial prefactors in Eq. (13) or the usage of "symmetry-adapted" floating geminals.[26,27]

Any linear transformation of the translationally invariant coordinates reads

$$(\boldsymbol{r},\boldsymbol{x}_0)^{\mathrm{T}} = (\boldsymbol{T}\otimes\boldsymbol{I}_3)(\tilde{\boldsymbol{r}},\boldsymbol{x}_0)^{\mathrm{T}}, \tag{16}$$

where

$$\begin{aligned}&(\boldsymbol{r},\boldsymbol{x}_0)^{\mathrm{T}} = (\boldsymbol{U}\otimes\boldsymbol{I}_3)\boldsymbol{x}, \quad (\tilde{\boldsymbol{r}},\boldsymbol{x}_0)^{\mathrm{T}} = (\tilde{\boldsymbol{U}}\otimes\boldsymbol{I}_3)\boldsymbol{x},\\ &\text{and}\quad \boldsymbol{T} = \boldsymbol{U}\tilde{\boldsymbol{U}}^{-1}.\end{aligned} \tag{17}$$

The basis functions can be written in terms of the "new" coordinates $\tilde{\boldsymbol{r}}$ as

$$\phi(\boldsymbol{r};\boldsymbol{C}) = \exp[-\boldsymbol{r}^{\mathrm{T}}(\boldsymbol{C}\otimes\boldsymbol{I}_3)\boldsymbol{r}] = \exp[-\tilde{\boldsymbol{r}}^{\mathrm{T}}(\tilde{\boldsymbol{C}}\otimes\boldsymbol{I}_3)\tilde{\boldsymbol{r}}], \tag{18}$$

where

$$\begin{pmatrix}\tilde{\boldsymbol{C}} & \boldsymbol{0}\\ \boldsymbol{0} & c\end{pmatrix} = \boldsymbol{T}^{\mathrm{T}}\begin{pmatrix}\boldsymbol{C} & \boldsymbol{0}\\ \boldsymbol{0} & c\end{pmatrix}\boldsymbol{T}. \tag{19}$$

This simple transformation property is exploited during the evaluation of matrix elements with (anti)symmetrized basis functions.

C. Analytic matrix elements

The integral of a spin-independent and permutationally invariant operator $\hat{O}$, corresponding to the Ith and Jth basis functions is now written as

$$\begin{aligned}O_{IJ} &= \langle\hat{\mathcal{A}}\{\phi(\boldsymbol{r};\boldsymbol{C}_I)\chi(\boldsymbol{\sigma};\boldsymbol{\theta}_I)\}|\hat{O}|\hat{\mathcal{A}}\{\phi(\boldsymbol{r};\boldsymbol{C}_J)\chi(\boldsymbol{\sigma};\boldsymbol{\theta}_J)\}\rangle\\ &= \sum_{p=1}^{N_{\text{perm}}}\varepsilon_p\langle\chi(\boldsymbol{\sigma};\boldsymbol{\theta}_I)|\hat{\mathcal{P}}_p\chi(\boldsymbol{\sigma};\boldsymbol{\theta}_J)\rangle\langle\phi(\boldsymbol{r};\boldsymbol{C}_I)|\hat{O}|\hat{\mathcal{P}}_p\phi(\boldsymbol{r};\boldsymbol{C}_J)\rangle\\ &= \sum_{p=1}^{N_{\text{perm}}}\kappa_{IJp}O_{IJp},\end{aligned} \tag{20}$$

where the quasi-idempotency of the (anti)symmetrizer, $\hat{\mathcal{A}}\hat{\mathcal{A}} = (N_{\text{perm}})^{1/2}\hat{\mathcal{A}}$, was exploited and the definitions

$$\kappa_{IJp} = \varepsilon_p\langle\chi(\boldsymbol{\sigma};\boldsymbol{\theta}_I)|\hat{\mathcal{P}}_p\chi(\boldsymbol{\sigma};\boldsymbol{\theta}_J)\rangle, \tag{21}$$

$$O_{IJp} = \langle\phi(\boldsymbol{r};\boldsymbol{C}_I)|\hat{O}|\hat{\mathcal{P}}_p\phi(\boldsymbol{r};\boldsymbol{C}_J)\rangle = \langle\phi(\boldsymbol{r};\boldsymbol{C}_I)|\hat{O}|\phi(\boldsymbol{r};\boldsymbol{C}_{Jp})\rangle, \tag{22}$$

were introduced. Note that the subscript p refers to the effect of the permutation operator $\hat{\mathcal{P}}_p$. The action of $\hat{\mathcal{P}}_p$ on the spin functions corresponds to the permutation of the elementary spin functions, and thus the evaluation of κ_{IJp} is straightforward. $\hat{O}$ is in this work either the unit operator or the translationally invariant Hamiltonian, and thus O_{IJp} corresponds to S_{IJp} or H_{IJp}, respectively.

As to the spatial part, the effect of the permutation operator is equivalent to a linear transformation of the translationally invariant Cartesian coordinates, which is accounted for through the transformation of the basis function coefficients explained earlier. The evaluation procedure of the overlap and the Hamiltonian matrix elements is outlined as follows.

For any two spatial basis functions denoted by $\phi(\boldsymbol{r};\boldsymbol{C}')$ and $\phi(\boldsymbol{r};\boldsymbol{C}'')$ the overlap and two integrals, which when multiplied by some constant factors correspond to the kinetic and the potential energy terms, are

$$s = \langle\phi(\boldsymbol{r};\boldsymbol{C}')|\phi(\boldsymbol{r};\boldsymbol{C}'')\rangle = \left(\frac{\pi^N}{\det\boldsymbol{\mathcal{C}}}\right)^{3/2}, \tag{23}$$

$$\langle\phi(\boldsymbol{r};\boldsymbol{C}')|\Delta_{\boldsymbol{r}_1}|\phi(\boldsymbol{r};\boldsymbol{C}'')\rangle = s\,6\mathrm{Tr}(\boldsymbol{\mathcal{C}}^{-1}\boldsymbol{C}'\boldsymbol{C}''), \tag{24}$$

$$\langle\phi(\boldsymbol{r};\boldsymbol{C}')|\frac{1}{|\boldsymbol{r}_1|}|\phi(\boldsymbol{r};\boldsymbol{C}'')\rangle = s\,\frac{2}{\sqrt{\pi\mathcal{C}_{11}}}, \tag{25}$$

where the notation $\boldsymbol{\mathcal{C}} = \boldsymbol{C}' + \boldsymbol{C}'' \in \mathbb{R}^{N\times N}$ was introduced for brevity. Thus, the evaluation of S_{IJp} is straightforward, while for H_{IJp} we proceed as follows.

Upon a linear transformation of the original set of translationally invariant Cartesian coordinates $\boldsymbol{r}$ to a new set $\tilde{\boldsymbol{r}}$, an integral transforms as

$$\begin{aligned}\langle\hat{o}(\boldsymbol{r})\rangle &= \langle\phi(\boldsymbol{r};\boldsymbol{C}')|\hat{o}(\boldsymbol{r})|\phi(\boldsymbol{r};\boldsymbol{C}'')\rangle\\ &= \int_{\mathbb{R}^{N\times 3}}\hat{o}(\boldsymbol{r})\exp[-\boldsymbol{r}^{\mathrm{T}}(\boldsymbol{\mathcal{C}}\otimes\boldsymbol{I}_3)\boldsymbol{r}]\mathrm{d}\boldsymbol{r}\\ &= [\det(\boldsymbol{T}^{\mathrm{T}}\boldsymbol{T})]^{3/2}\int_{\mathbb{R}^{N\times 3}}\hat{o}(\tilde{\boldsymbol{r}})\exp[-\tilde{\boldsymbol{r}}^{\mathrm{T}}(\tilde{\boldsymbol{C}}\otimes\boldsymbol{I}_3)\tilde{\boldsymbol{r}}]\mathrm{d}\tilde{\boldsymbol{r}}\\ &= [\det(\boldsymbol{T}^{\mathrm{T}}\boldsymbol{T})]^{3/2}\langle\hat{o}(\tilde{\boldsymbol{r}})\rangle,\end{aligned} \tag{26}$$

where $\tilde{\boldsymbol{C}}$ corresponds to the transformed $\boldsymbol{\mathcal{C}}$ according to Eq. (19).

As it is always possible to find an appropriate set of translationally invariant coordinates, in which the various terms of the Hamiltonian, Eq. (7), can be written in terms of $\Delta_{\boldsymbol{r}_1}$ and $1/|\boldsymbol{r}_1|$ (e.g., Jacobi and HPC coordinates in Eqs. (4) and (5)), the integrals H_{IJp} can be constructed entirely by using the primitive integrals, Eqs. (23) and (25), Eq. (26), and the coefficient matrices, $\tilde{\boldsymbol{C}}_I$ and $\tilde{\boldsymbol{C}}_{Jp}$, calculated according to Eq. (19).

D. Eigensolver and optimization of the basis function parameters

As the basis functions are non-orthogonal the generalized eigenvalue problem

$$\boldsymbol{H}\boldsymbol{c} = E\boldsymbol{S}\boldsymbol{c} \tag{27}$$

is to be solved. Eigenvalues, E, and eigenvectors, $\boldsymbol{c}$, are thus calculated using a "generalized" eigensolver. In order to generate or refine the basis set, the basis function parameters, here the exponents, are optimized in a stochastic variational procedure.[26,39–42] Due to the non-orthogonality of the basis functions possible near-linear dependency in the basis set is handled in the finite precision arithmetic of the computations by using Löwdin's canonical orthogonalization.[43] In practice, it is relatively straightforward to generate the basis function exponents so that they are well-distributed, and thus the near-linear dependency does not cause any numerical difficulty using 8-byte ("double precision" in Fortran) arithmetics.

III. PARTICLE DENSITIES

In the present all-particle calculations particles, i.e., electrons and nuclei, are handled on equal footing as quantum particles. In contrast to the clamped nucleus framework, the structural parameters do not have sharp, "dispersionless" values but they are characterized by some probability density. For states with $L = 0$ angular momentum and $p = +1$ parity the wave function, and thus the particle densities, are spherically symmetric. Furthermore, due to the quantum mechanical description, identical particles are indistinguishable. In order to be able to extract structural information from the all-particle wave function and to recognize classical molecular structural motifs, i.e., bonds and angles, we start out from the probabilistic interpretation of the wave function and calculate marginal probability densities.[44–47] Then, radial and angular probability densities will be derived from the marginal densities of selected particles, in order to obtain the probability density for the distances and angles of interest. In what follows a short overview of the most relevant literature is given and the density functions are introduced which are used in this work.

In Refs. 48 and 49, pseudoparticle one-densities were calculated in order to characterize the radial distribution of the particles. In Refs. 50 and 51, Ps_2 was analyzed by calculating the electron-electron and electron-positron correlation functions. In Ref. 25 the probability density distribution of the internuclear distance was calculated for vibrational states of H_2 and D_2, while in Ref. 52 the deuteron-proton correlation function was evaluated to demonstrate the charge asymmetry in vibrational states of HD.

In Ref. 20, $\{a, a, b\}$-type three-particle systems were studied within the Hooke–Calogero model and an atomic- to molecular-like topological transition was observed in the mass-density distribution of the a particles in terms of the variation of the mass of the constituent particles. In Ref. 21, $\{a^{\pm}, a^{\pm}, b^{\mp}\}$-type three-particle Coulomb-interacting systems were described within non-relativistic quantum mechanics and a similar atomic to molecular-type topological transition was observed in terms of the variation of the relative mass of the particles. Müller-Herold has already used the two-particle density to show the angular correlation between particles in a modified Hooke–Calogero model and observed a transition from helium-like angular correlation to directed bonding in terms of the variation of the masses of the constituent particles.[53]

In Refs. 54–56, the H^- ion was studied and the adiabatic two-density function indicated that the electrons take a bent V-shaped "triatomic molecule-like" arrangement in certain resonance states.

Finally, we note that within the BO approximation the structure of floppy systems with large amplitude motions cannot be characterized by relying on a single local minimum of the potential energy surface. Instead, it is more convenient to calculate the probability density for some internal coordinates.[57]

A. Particle density functions used in this study

According to the probabilistic interpretation of the wave function, one can analyze the simultaneous finding probability of some particles by calculating the joint or marginal probability density functions. The probability density of some selected particles measured with respect to some "center point" P fixed to the body is

$$\begin{aligned} &D^{(n)}_{P,a_1a_2\ldots a_n}(\boldsymbol{R}_1, \boldsymbol{R}_2, \ldots, \boldsymbol{R}_n) \\ &= \langle\Psi|\delta(\boldsymbol{x}_{a_1} - \boldsymbol{x}_P - \boldsymbol{R}_1)\delta(\boldsymbol{x}_{a_2} - \boldsymbol{x}_P - \boldsymbol{R}_2)\ldots \\ &\quad \times \delta(\boldsymbol{x}_{a_n} - \boldsymbol{x}_P - \boldsymbol{R}_n)|\Psi\rangle \end{aligned} \tag{28}$$

with $\boldsymbol{R}_i \in \mathbb{R}^3$ and the three-dimensional Dirac delta distribution, $\delta(\boldsymbol{z})$. In our calculations $n = 1$ or 2, the "a_i"s label particles, and the center point P is chosen to be either the center of mass (denoted by "0") or another particle. First, the density function

$$D^{(1)}_{P,a}(\boldsymbol{R}_1) = \langle\Psi|\delta(\boldsymbol{x}_a - \boldsymbol{x}_P - \boldsymbol{R}_1)|\Psi\rangle \tag{29}$$

is considered. For $P = 0$, $D^{(1)}_{0,a}$ characterizes the spatial distribution, localization or delocalization, of particle a with respect to the center of mass ("0"), while for $P = b$, $D^{(1)}_{b,a}$ measures the radial correlation between particles b and a.

Then, in order to identify the angular correlation of particles a and b with respect to P, the density function

$$D^{(2)}_{P,ab}(\boldsymbol{R}_1, \boldsymbol{R}_2) = \langle\Psi|\delta(\boldsymbol{x}_a - \boldsymbol{x}_P - \boldsymbol{R}_1)\delta(\boldsymbol{x}_b - \boldsymbol{x}_P - \boldsymbol{R}_2)|\Psi\rangle \tag{30}$$

will be calculated with the center point chosen to be the origin, $D^{(2)}_{0,ab}$, or another particle c, $D^{(2)}_{c,ab}$.

As the overall space rotation-inversion leaves the system invariant ($L = 0, p = +1$), it is sufficient to consider $D^{(1)}_{P,a}(\boldsymbol{R}_1)$ along a ray. Thus, for convenience,

$$\rho_{P,a}(R) = D^{(1)}_{P,a}(\boldsymbol{R}_1) \tag{31}$$

is introduced with $\boldsymbol{R}_1 = (0, 0, R)$ and $R \in \mathbb{R}^+_0$. Throughout this work the normalization is chosen according to

$$4\pi \int_0^\infty \mathrm{d}R\, R^2\, \rho_{P,a}(R) = 1. \tag{32}$$

As $D^{(2)}_{P,ab}(\boldsymbol{R}_1, \boldsymbol{R}_2)$ is also spherically symmetric ($L = 0, p = +1$), its actual value depends only on the lengths $R_1 = |\boldsymbol{R}_1|$ and $R_2 = |\boldsymbol{R}_2|$ and, for non-zero lengths, on the angle α of intersection of the vectors $\boldsymbol{R}_1$ and $\boldsymbol{R}_2$. In order to calculate the probability density for the angle α the radial dependence is integrated out and the "effective" angular density is defined as

$$\Gamma_{P,ab}(\alpha) = \int_0^\infty \mathrm{d}R_1 R_1^2 \int_0^\infty \mathrm{d}R_2 R_2^2\, D^{(2)}_{P,ab}(\boldsymbol{R}_1, \boldsymbol{R}_2). \tag{33}$$

Throughout this work the angular density is normalized according to

$$8\pi^2 \int_0^\pi \mathrm{d}\alpha \sin\alpha\, \Gamma_{P,ab}(\alpha) = 1. \tag{34}$$

B. Calculation of particle density functions

Using a normalized wave function expressed as a linear combination of the basis functions

$$\Psi = \sum_{I=1}^{N_\mathrm{b}} c_I \hat{\mathcal{A}}\{\phi(\boldsymbol{r}; \boldsymbol{C}_I)\chi(\boldsymbol{\sigma}; \boldsymbol{\theta}_I)\}, \tag{35}$$

the expectation value of a spin-independent density operator $\hat{\mathcal{D}}$ is given by

$$\begin{aligned} \mathcal{D} &= \langle\Psi|\hat{\mathcal{D}}|\Psi\rangle \\ &= \sum_{IJ=1}^{N_\mathrm{b}} c_I c_J \langle\hat{\mathcal{A}}\{\phi(\boldsymbol{r}; \boldsymbol{C}_I)\chi(\boldsymbol{\sigma}; \boldsymbol{\theta}_I)\}|\hat{\mathcal{D}}|\hat{\mathcal{A}}\{\phi(\boldsymbol{r}; \boldsymbol{C}_J)\chi(\boldsymbol{\sigma}; \boldsymbol{\theta}_J)\}\rangle \\ &= \sum_{IJ=1}^{N_\mathrm{b}} \sum_{pr=1}^{N_\mathrm{perm}} c_I c_J \frac{\varepsilon_p \varepsilon_r}{N_\mathrm{perm}} \\ &\quad \times \langle\hat{\mathcal{P}}_p\{\phi(\boldsymbol{r}; \boldsymbol{C}_I)\chi(\boldsymbol{\sigma}; \boldsymbol{\theta}_I)\}|\hat{\mathcal{D}}|\hat{\mathcal{P}}_r\{\phi(\boldsymbol{r}; \boldsymbol{C}_J)\chi(\boldsymbol{\sigma}; \boldsymbol{\theta}_J)\}\rangle \\ &= \sum_{IJ=1}^{N_\mathrm{b}} \sum_{pr=1}^{N_\mathrm{perm}} c_I c_J \frac{\varepsilon_p \varepsilon_r \kappa_{IJpr}}{N_\mathrm{perm}} \mathcal{D}_{IJpr}, \end{aligned} \tag{36}$$

where the shorthand notations

$$\kappa_{IJpr} = \langle\hat{\mathcal{P}}_p\chi(\boldsymbol{\sigma}; \boldsymbol{\theta}_I)|\hat{\mathcal{P}}_r\chi(\boldsymbol{\sigma}; \boldsymbol{\theta}_J)\rangle \tag{37}$$

and

$$\begin{aligned} \mathcal{D}_{IJpr} &= \langle\hat{\mathcal{P}}_p\phi(\boldsymbol{r}; \boldsymbol{C}_I)|\hat{\mathcal{D}}|\hat{\mathcal{P}}_r\phi(\boldsymbol{r}; \boldsymbol{C}_J)\rangle \\ &= \langle\phi(\boldsymbol{r}; \boldsymbol{C}_{Ip})|\hat{\mathcal{D}}|\phi(\boldsymbol{r}; \boldsymbol{C}_{Jr})\rangle \end{aligned} \tag{38}$$

were introduced. Note that the $\hat{\mathcal{D}}$-type operators as introduced in Eqs. (29) and (30) might not be permutationally invariant. Nevertheless, the calculation according to Eq. (36), using the (anti)symmetrized basis function expansion, guarantees that the resulting density function is invariant under the permutation of identical particles. The density functions defined in this work are normalized to one. In numerical calculations (Sec. IV), the requirements of the permutation invariance and unit normalization were tested and fulfilled, as required by the theory.

Evaluation of the spin-permutation coefficient, κ_{IJpr}, is straightforward, see Sec. II C. In order to calculate the $\mathcal{D}_{IJpr}$ terms for the particle densities defined in Eqs. (29) and (30), it is sufficient to consider the integrals for one- and two-density operators written in the general form of

$$\hat{\mathcal{D}}^{(1)} = \delta(\tilde{\boldsymbol{r}}_1 - \boldsymbol{R}_1) \tag{39}$$

or

$$\hat{\mathcal{D}}^{(2)} = \delta(\tilde{\boldsymbol{r}}_1 - \boldsymbol{R}_1)\delta(\tilde{\boldsymbol{r}}_2 - \boldsymbol{R}_2), \tag{40}$$

respectively. It is always possible to construct translationally invariant coordinates so that $\tilde{\boldsymbol{r}}_1 = \boldsymbol{x}_{a_1} - \boldsymbol{x}_P$ and $\tilde{\boldsymbol{r}}_2 = \boldsymbol{x}_{a_2} - \boldsymbol{x}_P$. If P is the center of mass, then $\tilde{\boldsymbol{r}}_i$s will be the "center-of-mass centered" coordinates, Eq. (6), and if P is fixed to a particle, then $\tilde{\boldsymbol{r}}_i$s will be the "heavy-particle centered" coordinates, Eq. (5).

Then, the density functions can be constructed according to Sec. II C and using the "primitive integrals" of

$\hat{d}^{(1)} = \delta(\boldsymbol{r}_1 - \boldsymbol{R}_1)$ and $\hat{d}^{(2)} = \delta(\boldsymbol{r}_1 - \boldsymbol{R}_1)\delta(\boldsymbol{r}_2 - \boldsymbol{R}_2)$ for any two spatial basis functions, $\phi(\boldsymbol{r}; \boldsymbol{C}')$ and $\phi(\boldsymbol{r}; \boldsymbol{C}'')$ ($N > n$):

$$d^{(n)} = \langle \phi(\boldsymbol{r}; \boldsymbol{C}') | \hat{d}^{(n)} | \phi(\boldsymbol{r}; \boldsymbol{C}'') \rangle = f_0 \exp\left[- \sum_{i,j=1}^{n} \beta_{ij}^{(n)} \boldsymbol{R}_i^{\mathrm{T}} \boldsymbol{R}_j \right] \tag{41}$$

with

$$f_0 = \left(\frac{\pi^{N-n}}{\det \boldsymbol{\Omega}^{(n)}} \right)^{\frac{3}{2}} \tag{42}$$

and

$$\beta_{ij}^{(n)} = \mathcal{C}_{ij} - \boldsymbol{\omega}_i^{(n)\mathrm{T}} \boldsymbol{\Omega}^{(n)-1} \boldsymbol{\omega}_j^{(n)}, \quad i, j = 1, \ldots, n, \quad n = 1, 2, \tag{43}$$

where $\boldsymbol{\mathcal{C}} = \boldsymbol{C}' + \boldsymbol{C}'' \in \mathbb{R}^N \times N$, $\boldsymbol{\omega}_i^{(n)} \in \mathbb{R}^{N-n}$ contains the last $N - n$ elements of the ith column of $\boldsymbol{\mathcal{C}}$, and $\boldsymbol{\Omega}^{(n)}$ is the right-lower $(N - n) \times (N - n)$ block of $\boldsymbol{\mathcal{C}}$. Note that for the case of $N = n$ (the case of $N + 1 = 3$ and $n = 2$ in Sec. IV) $d^{(n)}$ is obtained as the absolute square of the basis function, expressed in the appropriate coordinates, and no integration is necessary. Then, $d^{(2)}$ has a similar form as in Eq. (41) with $f_0 = 1$ and $\beta_{ij}^{(2)} = \mathcal{C}_{ij}$.

Finally, using the expression for $d^{(2)}(\boldsymbol{R}_1, \boldsymbol{R}_2)$ the evaluation of the angular density, $\Gamma_{P,ab}$, is straightforward by integrating over the radial coordinates, R_1 and R_2. The corresponding "primitive" integral is given in the Appendix and is used for the numerical evaluation of $\Gamma_{P,ab}$ (Sec. IV).

IV. NUMERICAL RESULTS

All-particle wave functions for the ground states with $L = 0$ angular momentum and $p = +1$ parity of the three-particle H^- ($S_e = 0$, singlet), Ps^- ($S_{e^-} = 0$), and H_2^+ ($S_p = 0$, para), the four-particle Ps_2 ($S_{e^\pm} = 0$) and H_2 ($S_e = 0$, singlet; $S_p = 0$, para), as well as the five-particle H_2D^+ ($S_e = 0$, singlet; $S_p = 0$, para) were calculated and analyzed using radial and angular densities derived from n-particle densities (Sec. III). The mass ratios $m_p/m_e = 1836.15267247$ and $m_d/m_e = 3670.4829654$ (Ref. 58) were used throughout the calculations, and e (or e^-/e^+), p, and d refer to the electron/positron, proton, and the deuteron, respectively. The center of mass is denoted by "0".

In Table I the energies and virial coefficients are given for the ground-state wave functions calculated and used for the generation of the density plots shown in Figures 1–7. At the end of this section a short overview of the convergence properties of the radial and angular densities is given. Interestingly, the main elements of molecular structure can be recognized relatively "early" during the course of the convergence of the total energy. Note that the total energy does not need to be converged very tightly in order to recognize the important characteristics of the particle densities as we shall see.

TABLE I. Energies and virial coefficients of the calculated ground-state wave functions used for the evaluation of the probability densities shown in Figures 1–7.

Species	E / E_h	δ [a] / E_h	$1 + \langle \hat{V} \rangle / 2\langle \hat{T} \rangle$
H^-	−0.5274	2×10^{-7}	-2.6×10^{-7}
Ps^-	−0.2620	9×10^{-8}	-8.8×10^{-8}
H_2^+	−0.5971	6×10^{-5}	-6.7×10^{-5}
Ps_2	−0.5160	2×10^{-7}	-2.4×10^{-7}
H_2	−1.1640	6×10^{-5}	-8.9×10^{-5}
H_2D^+	−1.3173	5×10^{-3}	-3.5×10^{-3}

[a] $\delta = E(\mathrm{Ref.}) - E$. The reference energies, E(Ref.), are taken from Refs. 59–63 and 48 for H^-, Ps^-, H_2^+, Ps_2, H_2, and H_2D^+, respectively.

A. Radial density

As all particles, electrons and nuclei, are handled on equal footing as quantum particles the structural parameters do not have sharp values but are characterized by some probability distributions. The one-particle densities calculated with respect to the center of mass of the system provide some insight in the distribution of the particles, and thus the structure of the system. Due to the spherical symmetry, the one-particle density depends only on the distance of the particle from the center of mass, R, and is independent of the orientation. In Figures 1 and 2 the radial densities, $\rho_{0,a}(R)$, are shown for three-, four-, and five-particle systems (a denotes the particle and "0" means that the origin is the center of mass). For example, the proton density with respect to the center of mass in H_2D^+, Figure 2, is defined as

$$\rho_{0,\mathrm{p}}(R) = \langle \Psi | \delta(\boldsymbol{x}_\mathrm{p} - \boldsymbol{x}_0 - \boldsymbol{R}_1) | \Psi \rangle \tag{44}$$

with $\boldsymbol{R}_1 = (R, 0, 0)$. Note that indistinguishability of identical particles holds, and thus, for instance, $\rho_{0,\mathrm{p}} = \rho_{0,\mathrm{p}'}$.

Figure 1 shows qualitatively different $\rho_{0,a}(R)$ density profiles in $\{a^\pm, a^\pm, b^\mp\}$-type three-particle systems for various m_a/m_b values. In Ref. 21 we presented the transition of $\rho_{0,a}$ from a center-of-mass centered, "atom-like" to a "shell-like" density function by increasing the m_a/m_b ratio. This "alchemical transformation involving the mass"[64] allowed us to observe the emergence of molecular structure in these simple systems (also note the mass-scale similarity and the charge inversion symmetry described in Ref. 21). Interestingly, the density of the third particle remains center-of-mass centered and only its dispersion increases as m_a/m_b increases, Figure 1. The qualitative properties of the particle density of both the equal particles and the third particle are similar to those of the Hooke–Calogero model.[20]

As to larger systems, Figure 2 shows one-particle densities, $\rho_{0,a}$ for H_2, Ps_2, and H_2D^+. Similar to the three-particle case, the heavy particles, here nuclei, form shells around the center of mass ($L = 0, p = +1$), while the light particles, here electrons, have a broader density function with a maximum at the center of mass.

The effect of the Coulomb repulsion and attraction can be directly observed in the particle-particle correlation functions, $\rho_{b,a}(R)$, shown in Figure 3. For example, the d-p or p-p′ correlation functions in H_2D^+ are defined as

$$\rho_{\mathrm{d,p}}(R) = \langle \Psi | \delta(\boldsymbol{x}_\mathrm{p} - \boldsymbol{x}_\mathrm{d} - \boldsymbol{R}_1) | \Psi \rangle, \tag{45}$$

$$\rho_{\mathrm{p,p}'}(R) = \langle \Psi | \delta(\boldsymbol{x}_\mathrm{p} - \boldsymbol{x}_{\mathrm{p}'} - \boldsymbol{R}_1) | \Psi \rangle \tag{46}$$

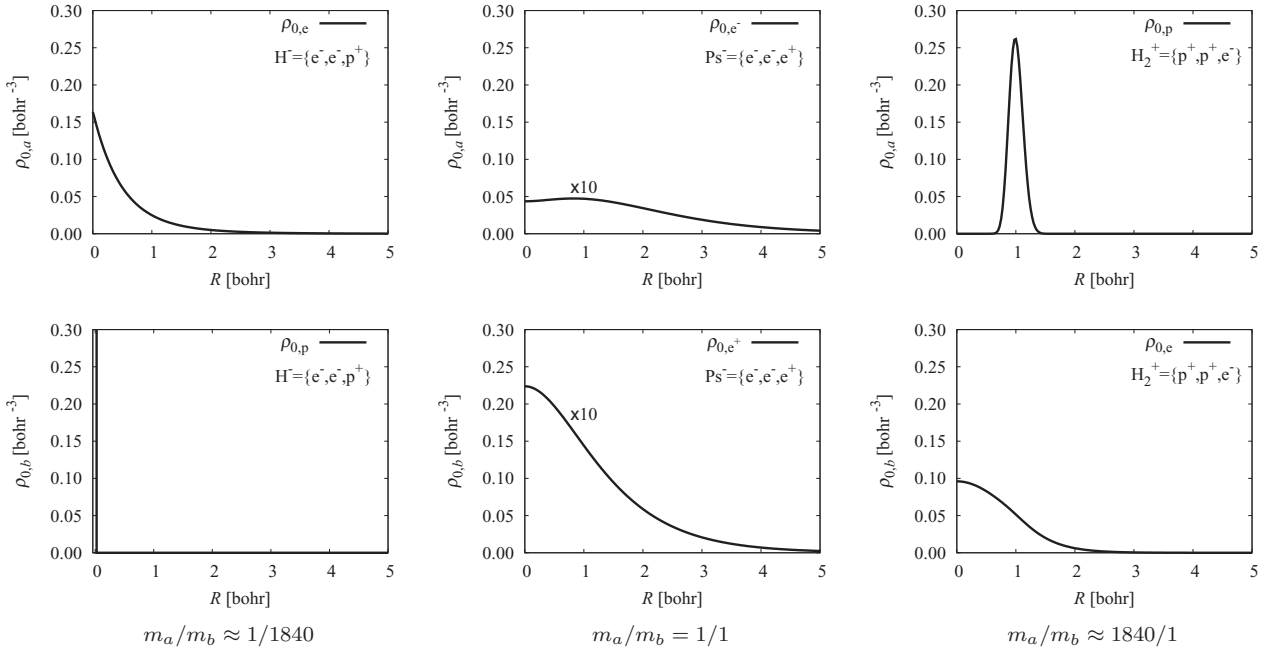

FIG. 1. One-particle densities, $\rho_{0,a}(R)$, in $\{a^{\pm}, a^{\pm}, b^{\mp}\}$-type three-particle systems. The normalization is chosen according to $4\pi \int_0^\infty \mathrm{d}R\, R^2 \rho_{0,a}(R) = 1$. Note that $\rho_{0,\mathrm{p}}$ in H^- has a much larger maximum value at the origin than the largest value shown here. ρ_{0,e^-} and ρ_{0,e^+} of Ps^- are scaled up by a factor of 10 for the sake of a better comparison with the other systems.

with $\boldsymbol{R}_1 = (R, 0, 0)$. Furthermore, the particle-particle correlation functions provide direct information on the probability density for the distance of particles a and b.

Besides the Coulomb interaction, the decisive role of the masses in the formation of structural motifs is indicated by the qualitative change of the radial densities, Figures 1 and 2. Woolley,[6] Fröman and Kinsey,[65] as well as Lin *et al.*[66,67] suggested that the role of the mass of the particles could be understood by considering the mass-polarization terms in the translationally invariant Hamiltonian. The mass-polarization terms are the cross derivative terms in Eq. (7), which are non-vanishing due to the non-zero off-diagonal elements M_{kl} for non-orthogonal translationally invariant coordinates, $\boldsymbol{r}$. If the translationally invariant coordinates are chosen in

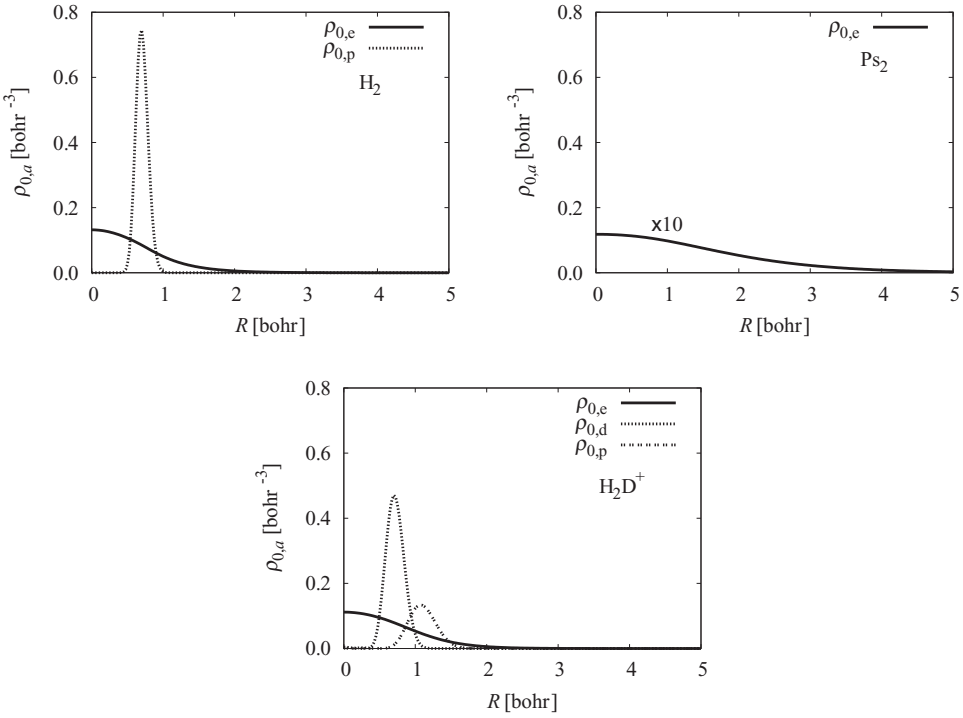

FIG. 2. One-particle densities, $\rho_{0,a}(R)$, for four- and five-particle systems. The normalization is chosen according to $4\pi \int_0^\infty \mathrm{d}R\, R^2 \rho_{0,a}(R) = 1$. Note that $\rho_{0,\mathrm{e}}$ of Ps_2 is scaled up by a factor of 10 for the sake of a better comparison with the other systems.

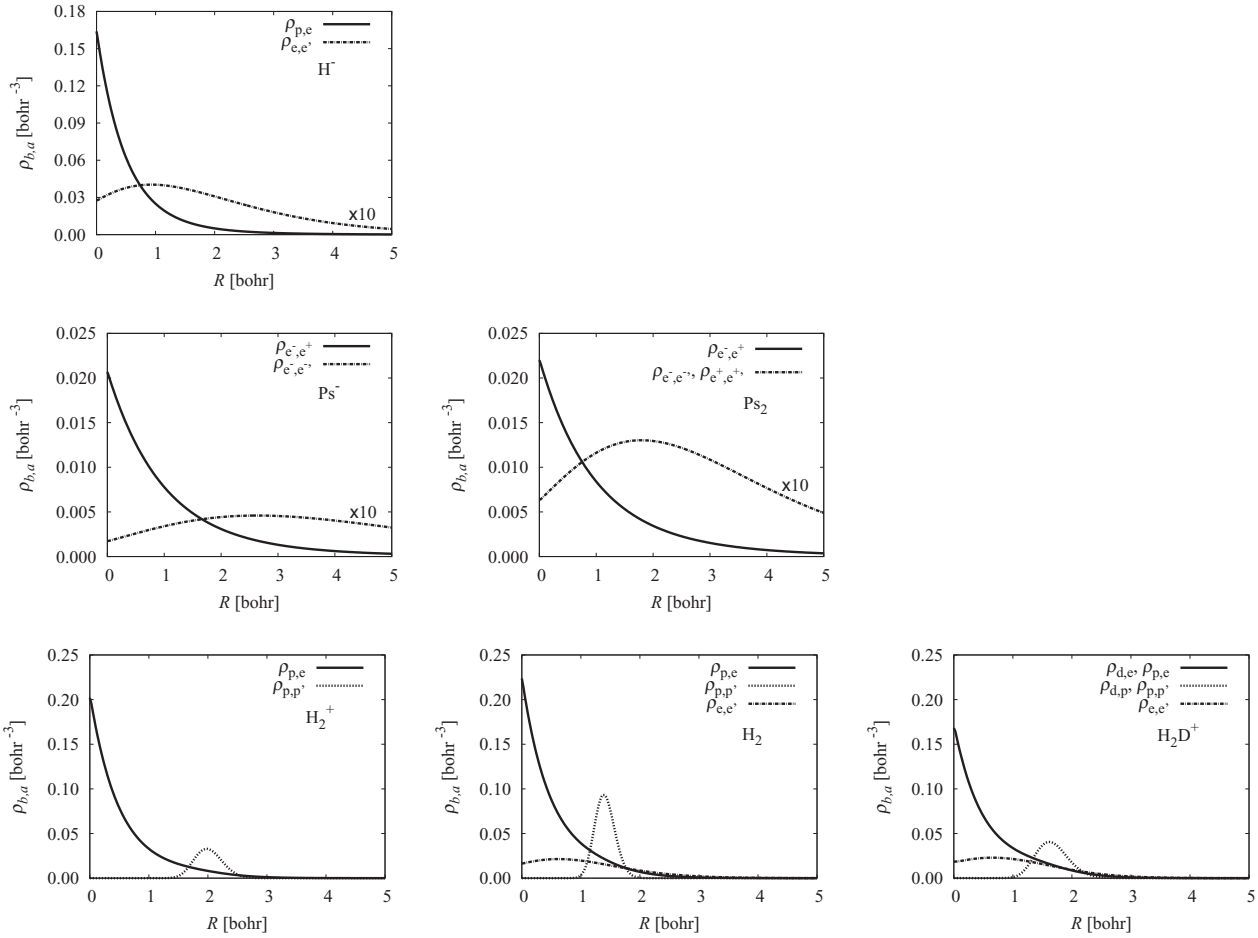

FIG. 3. Particle-particle correlation functions, $\rho_{b,a}(R)$, characterizing the probability density for particle-particle distances. The normalization is chosen according to $4\pi \int_0^\infty \mathrm{d}R\ R^2 \rho_{b,a}(R) = 1$. Note that $\rho_{e^-,e^{-\prime}}$ and $\rho_{e^+,e^{+\prime}}$ of Ps^- and Ps_2 are scaled up by a factor of 10 for the sake of a better comparison with the other systems.

$\{a^\pm, a^\pm, b^\mp\}$-type systems as the displacement vectors of particles b and a, and particles b and a', then for the hydride ion (or for the helium atom) the coefficients of the cross derivative terms are small, while, for example, for the case of H_2^+ (with a = p and b = e) they are substantial. Thus, the qualitative differences of the particle densities in systems with very different mass ratios, Figures 1 and 2, can be understood as mass-polarization "effects."

B. Angular density

The value of the relative mass, and thus the mass polarization, influences not only the radial distribution of the particles, but also their angular distribution. The angular density, $\Gamma_{c,\,ab}(\alpha)$, providing the probability density of the included angle α for a-c-b, is obtained by integrating $D_{c,ab}(\boldsymbol{R}_1, \boldsymbol{R}_1)$, over the radial variables, i.e., for the c-a and c-b distances.

For example, the angular density of the two protons with respect to the center of mass in H_2 is defined as

$$\Gamma_{0,\mathrm{pp}'}(\alpha) = \int_0^\infty \mathrm{d}R_1 R_1^2 \int_0^\infty \mathrm{d}R_2 R_2^2 \times \langle \Psi | \delta(\boldsymbol{x}_\mathrm{p} - \boldsymbol{x}_0 - \boldsymbol{R}_1)\delta(\boldsymbol{x}_{\mathrm{p}'} - \boldsymbol{x}_0 - \boldsymbol{R}_2) | \Psi \rangle, \tag{47}$$

while the angular density of the two electrons with respect to the positron in Ps^- is

$$\Gamma_{\mathrm{e}^+,\mathrm{e}^-\mathrm{e}^{-\prime}}(\alpha) = \int_0^\infty \mathrm{d}R_1 R_1^2 \int_0^\infty \mathrm{d}R_2 R_2^2 \times \langle \Psi | \delta(\boldsymbol{x}_{\mathrm{e}^-} - \boldsymbol{x}_{\mathrm{e}^+} - \boldsymbol{R}_1)\delta(\boldsymbol{x}_{\mathrm{e}^{-\prime}} - \boldsymbol{x}_{\mathrm{e}^+} - \boldsymbol{R}_2) | \Psi \rangle \tag{48}$$

with $\alpha \in [0, \pi]$ and $R_1 = |\boldsymbol{R}_1|$ and $R_2 = |\boldsymbol{R}_2|$. Note that the indistinguishability of identical particles holds, and thus, for instance, $\Gamma_{\mathrm{e}^+,\mathrm{e}^-\mathrm{e}^{-\prime}}(\alpha) = \Gamma_{\mathrm{e}^+,\mathrm{e}^{-\prime}\mathrm{e}^-}(\alpha)$.

The "effective" angular density measured with respect to the center of mass ("0"), $\Gamma_{0,aa'}$, is shown in Figure 4 for $\{a^\pm, a^\pm, b^\mp\}$-type three- and $\{a^\pm, a^\pm, b^\mp, b^\mp\}$-type four-particle systems. The figures show that the angular density of the equal particles, as it is seen from the center of mass, transforms from an "atomic-like" Coulomb-hole profile to a molecular-like rotating dumbbell ($L = 0$, $p = +1$) as m_a/m_b is increased. All densities calculated were normalized to 1 and the dotted line represents constant angular density corresponding to the idealized case of no angular correlation. The electrons in the H_2 molecule have an angular density profile (referenced to the center of mass), similar to the atomic case, in line with earlier suggestions, for example, by Woolley.[6] Similar to the case of the radial density, Fröman

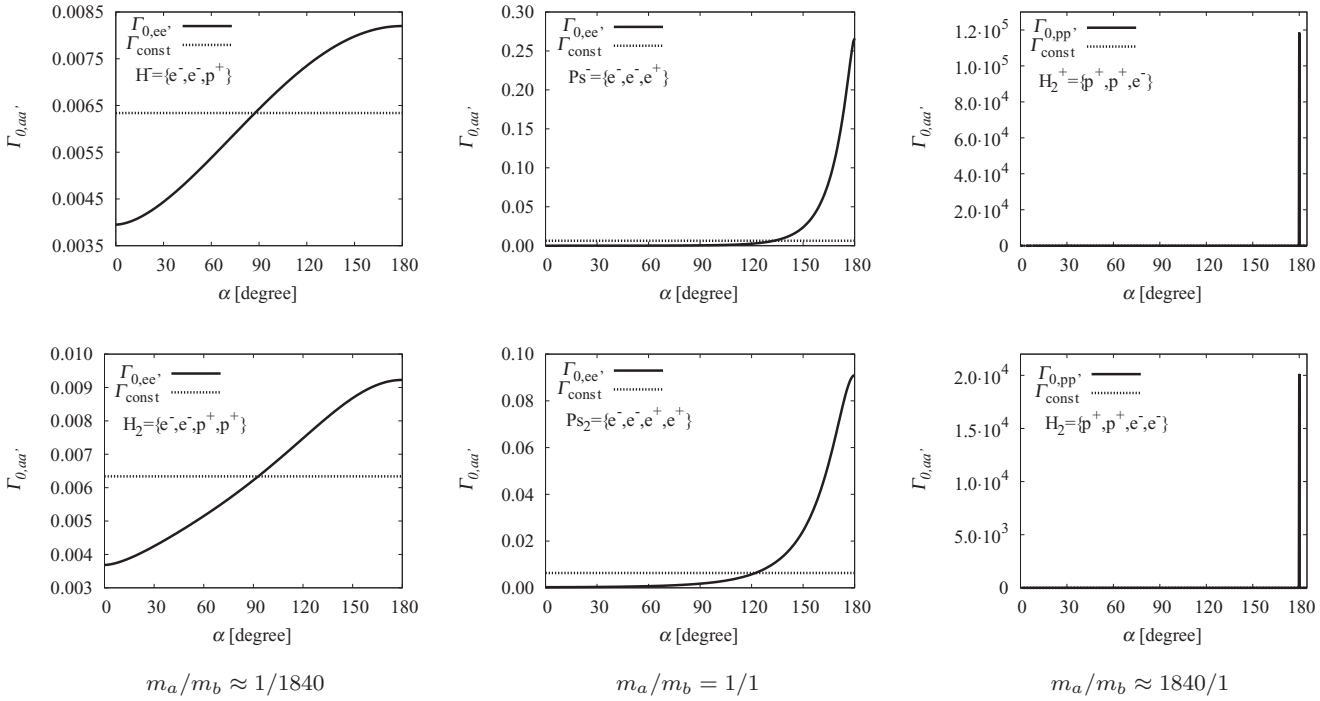

FIG. 4. Probability density of the a-0-a' included angle, $\Gamma_{0,aa'}(\alpha)$, in $\{a^{\pm}, a^{\pm}, b^{\mp}\}$- and $\{a^{\pm}, a^{\pm}, b^{\mp}, b^{\mp}\}$-type three- and four-particle systems, respectively. The angular density is normalized according to $8\pi^2 \int_0^{\pi} d\alpha \sin\alpha\ \Gamma_{0,aa'}(\alpha) = 1$. The hypothetical case of no angular correlation corresponds to $\Gamma_{\text{const}} = 1/16\pi^2 \approx 0.0063$, which is indicated by the dotted line in the plots.

and Kinsey argued[65] that the mass-polarization contribution would "overcome" the Coulomb contribution and this results in a probability density with a very large maximum for the p-0-p′ angle at 180° in the molecular systems, H_2^+ and H_2.

Besides the distribution of the particles in space, referenced to the center of mass, inspection of the particle-particle correlations provides insight in the "structure" of the system and allows us to extract information on bond angles. Figure 5 shows the probability density of the included angle for a-b-a'. The profile of $\Gamma_{b,aa'}$ shows a qualitative change as the value m_a/m_b increases. In line with the one-particle density, the angular density profile also indicates that $Ps^- = \{e^-, e^-, e^+\}$ is more "molecular" than atomic. In fact, the small maximum of the density for the e^--e^+-e^- angle near 60° indicates some directed bonding character, while the system is very delocalized or floppy indicated by the flat angular density curve with the small maximum value compared to the "uncorrelated" hypothetical case (Γ_{const}). A similar transition from an atomic, helium-like angular correlation to a directed bonding-type one was identified by one of us for the Hooke–Calogero model of three-particle systems.[53]

C. A simple numerical example for directed bonding

Motivated by the observation of the weak angular correlation observed in Ps^- with a "floppy" V-like structure, Figure 5, we considered a simple case where the more pronounced appearance of directed bonding could be anticipated.

Figure 6 shows the probability density for the p-d-p′ angle in H_2D^+. Although the wave function is not tightly

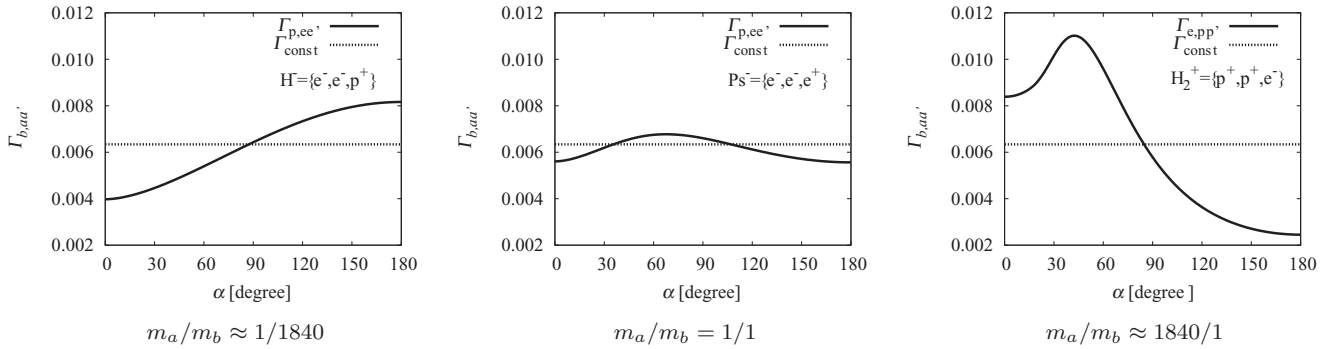

FIG. 5. Probability density of the a-b-a' included angle, $\Gamma_{b,aa'}(\alpha)$, in $\{a^{\pm}, a^{\pm}, b^{\mp}\}$-type three-particle systems. The angular density is normalized according to $8\pi^2 \int_0^{\pi} d\alpha \sin\alpha\ \Gamma_{b,aa'}(\alpha) = 1$. The hypothetical case of no angular correlation corresponds to $\Gamma_{\text{const}} = 1/16\pi^2 \approx 0.0063$, which is indicated by the dotted line in the plots.

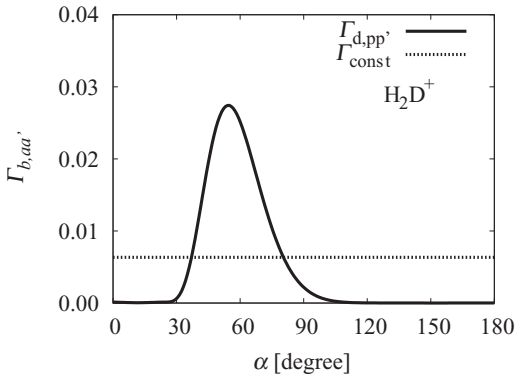

FIG. 6. Probability density of the p-d-p′ included angle, $\Gamma_{d,pp'}(\alpha)$, in the ground state of H_2D^+. The angular density is normalized according to $8\pi^2 \int_0^\pi d\alpha \sin\alpha\ \Gamma_{d,pp'}(\alpha) = 1$. The hypothetical case of no angular correlation corresponds to $\Gamma_{const} = 1/16\pi^2 \approx 0.0063$, which is indicated by the dotted line in the plots.

converged (see Table I), the angular density clearly shows a large maximum near 60° and it takes near zero values near 0° and 180°, which is, of course, in agreement with the Born–Oppenheimer description of this molecular ion. The maximum value in this case is much larger than that of Ps^- in Figure 5, which indicates a more "rigid" V-like structure.

It is also insightful to consider the angular density with respect to the center of mass, Figure 7. As to the electrons, $\Gamma_{0,ee'}$ has a helium-like Coulomb-hole profile. At the same time, the angular densities for the two protons and the deuteron and a proton show localized peaks near 90° and 130°, respectively, which indicates a pronounced angular correlation for the nuclei within the proton and deuteron shells around the center of mass.

Although the all-particle wave function representing the system is symmetric to space rotation and inversion ($L = 0, p = +1$) and fulfills the Pauli principle for the identical particles, the radial, Figures 1 and 2, and the angular densities, Figures 6 and 7, allow us to reconstruct or "extract," at least elements of, the traditional molecular structure.

D. Convergence of the radial and angular densities

Finally, a few remarks on the convergence properties of the studied radial and angular densities are in order. Numerical examples are shown in Figure 8 for the radial proton densities, $\rho_{0,p}$, in H_2 and H_2D^+, as well as for the angular densities of d-0-p, $\Gamma_{0,dp}$, and p-d-p′, $\Gamma_{d,pp'}$, in H_2D^+. The total energies corresponding to the wave functions used to calculate the densities are given in the top corner of each plot. Figure 8 shows that the main features of the radial and angular densities considered here—and which are related to the structural elements of molecular structure, i.e., bonds and angles—appeared relatively early during the course of the convergence of the energy.

V. SUMMARY AND CONCLUSION

The reconstruction of classical molecular structural motifs from the ground-state solution of the all-particle Schrödinger equation without the introduction of the Born–Oppenheimer approximation was investigated. If the nuclei are not fixed, the structural parameters are characterized with some probability density instead of a dispersionless sharp value. Thus, our analysis started out from the probabilistic interpretation of the all-particle wave function, *n*-particle density functions were evaluated, and radial and angular probability densities were derived from them. The classical structural motifs were identified as some arrangement of the relevant particles corresponding to large probabilities.

This program was first suggested at the conceptual level at least as early as in 1980 by Claverie and Diner[44] and was reviewed, for instance, in Ref. 46. It was later pursued by Müller-Herold for the Hooke–Calogero model,[20,53] and was carried out in the present work at the numerical level for some simple systems composed of particles with various masses. As a result, one- and two-dimensional motifs of molecular structure were identified in the ground-state all-particle wave functions ($L = 0, p = +1$), and the decisive role of the relative mass of the particles in the formation of structural motifs has been demonstrated. The procedure may be easily extended to three-dimensional structural elements and conceptual questions related to chirality[6,19,68–70] might also be addressed.

In general, *n*-point densities, i.e., joint or marginal probability distribution functions of a few variables, and related correlation functions are often used for the identification of typical patterns in various systems with many variables. For example, particle densities and correlation functions are used to describe not only the atomistic details of bulk materials in statistical mechanics[71] but also the large-scale structure of the

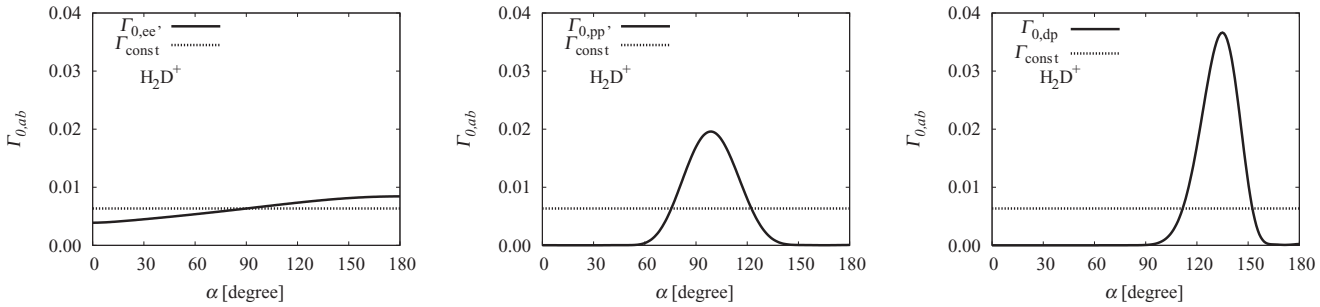

FIG. 7. Angular density, $\Gamma_{0,ab}(\alpha)$, characterizing the distribution of particles in the ground state of H_2D^+ around the center of mass. Note that the angular density is normalized according to $8\pi^2 \int_0^\pi d\alpha \sin\alpha\ \Gamma_{0,ab}(\alpha) = 1$. Thus, the hypothetical case of no angular correlation corresponds to $\Gamma_{const} = 1/16\pi^2 \approx 0.0063$ and is indicated by the dotted line.

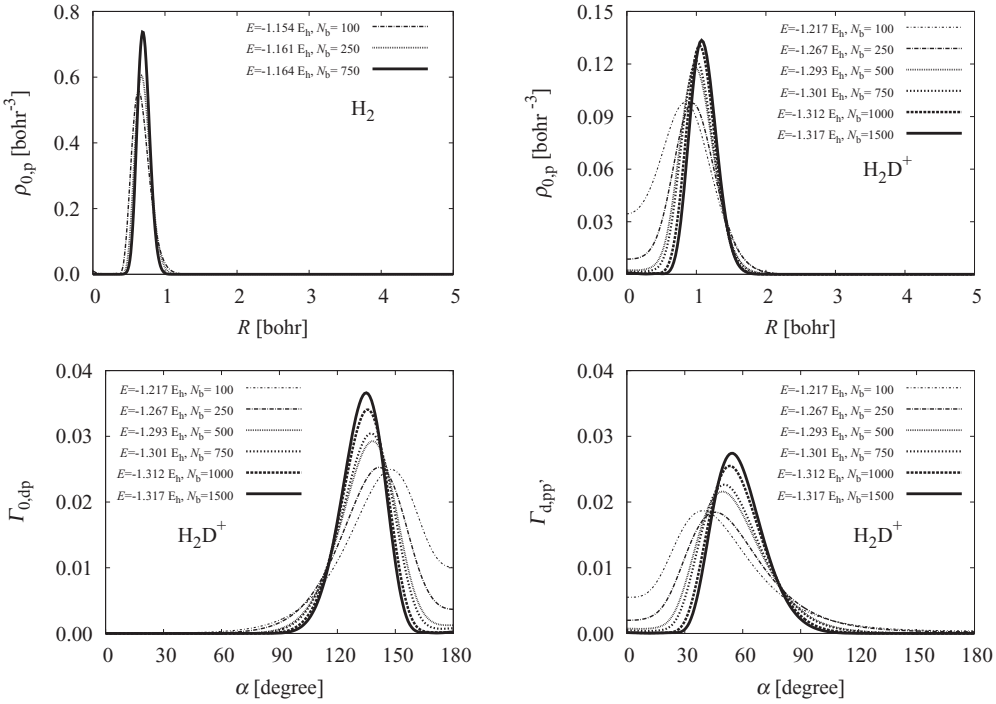

FIG. 8. Convergence of radial and angular densities. The densities shown here were calculated with various wave functions, obtained with varying numerical effort, and correspond to a total energy given in the top corner of each plot.

Universe in cosmology.[72] Although the analogy at the technical level exists, one has to distinguish between the statistical description of bulk materials and the probabilistic framework of quantum mechanics. While in bulk materials the statistical distribution of the multitude of various distinct structures is considered, the molecular wave function corresponds to the "superposition" of arrangements of the particles attached with some probabilities. It is interesting enough, that the main features of this "quantum"[44] structure of molecules can often be grasped in terms of classical molecular structural motifs.

While *motifs* or *elements* of molecular structure could be identified in the all-particle wave function of an isolated system, the wave function was not reduced to the *classical* ball-and-stick molecular model. For example, the V-shaped arrangement of the two protons and the deuteron in H_2D^+ was identified as a large maximum in the angular density of the nuclei, but the overall ground-state particle densities were ball-shaped due to space-rotation invariance, and thus, the classical triangular picture of the nuclear framework does not automatically arise from the quantum mechanical calculations. The related quantum-classical reduction problem was not addressed in the present work but it was analyzed carefully by Woolley[24,73] and Primas.[19] Actually, the fine interplay of the micro-scale manifestation of classical as well as the macro-scale survival of quantum effects is a peculiarity of the molecular world[74] and has probably a central role in a molecular-level understanding of matter or even life.

ACKNOWLEDGMENTS

E.M. acknowledges funding by an ETH Fellowship.

APPENDIX: CALCULATION OF THE ANGULAR DENSITY

The angular density was defined, Eq. (33), as

$$\Gamma(\alpha) = \int_0^\infty \mathrm{d}R_1 R_1^2 \int_0^\infty \mathrm{d}R_2 R_2^2 \; D^{(2)}(\boldsymbol{R}_1, \boldsymbol{R}_2) \tag{A1}$$

with

$$D^{(2)}(\boldsymbol{R}_1, \boldsymbol{R}_2) = \langle \Psi | \delta(\tilde{\boldsymbol{r}}_1 - \boldsymbol{R}_1) \delta(\tilde{\boldsymbol{r}}_2 - \boldsymbol{R}_2) | \Psi \rangle \; . \tag{A2}$$

The evaluation of $\Gamma(\alpha)$ proceeds similarly to that of $D^{(2)}(\boldsymbol{R}_1, \boldsymbol{R}_2)$ described in Sec. III B, but the function in Eq. (41),

$$d^{(2)}(\boldsymbol{R}_1, \boldsymbol{R}_2) = f_0 \; \exp\left[-\beta_{11}^{(2)} R_1^2 - \beta_{22}^{(2)} R_2^2 - 2\beta_{12}^{(2)} R_1 R_2 \cos\alpha\right], \tag{A3}$$

has to replaced by

$$\begin{aligned}
\gamma(\alpha) &= \int_0^\infty \mathrm{d}R_1 R_1^2 \int_0^\infty \mathrm{d}R_2 R_2^2 \; d^{(2)}(\boldsymbol{R}_1, \boldsymbol{R}_2) \\
&= f_0 \int_0^\infty \mathrm{d}R_1 R_1^2 \int_0^\infty \mathrm{d}R_2 R_2^2 \\
&\quad \times \exp\left[-\beta_{11}^{(2)} R_1^2 - \beta_{22}^{(2)} R_2^2 - 2\beta_{12}^{(2)} R_1 R_2 \cos\alpha\right] \\
&= f_0 \left\{ \frac{1}{8d^{3/2}} \left(1 + \frac{3a^2}{d}\right) \left[\frac{\pi}{2} - \arctan\left(\frac{a}{\sqrt{d}}\right)\right] \right. \\
&\quad \left. - \frac{a}{8bd}\left(1 + \frac{5a^2}{d}\right) + \frac{a}{4b^2}\left[-1 + \left(\frac{a^2}{d}\right)^2\right] \right\}
\end{aligned} \tag{A4}$$

with

$$a = \beta_{12}^{(2)} \cos\alpha, \quad b = \beta_{11}^{(2)} \beta_{22}^{(2)}, \quad d = b - a^2 , \qquad \text{(A5)}$$

where $\phi(\boldsymbol{r}; \boldsymbol{C}')$ and $\phi(\boldsymbol{r}; \boldsymbol{C}'')$ are two arbitrary spatial basis functions and f_0 and $\beta_{ij}^{(2)}$ have the same meaning as introduced below Eq. (41).

[1] U. Klein, *Experiments, Models, Paper Tools. Cultures of Organic Chemistry in the Nineteenth Century* (Stanford University Press, Stanford, 2003).
[2] A. J. Rocke, *Image & Reality: Kekulé, Kopp, and the Scientific Imagination (Synthesis)*, A Series in the History of Chemistry (University of Chicago, Chichago, 2010).
[3] W. Heitler and F. London, Z. Phys. **44**, 455 (1927).
[4] M. Born and R. Oppenheimer, Ann. Phys. **84**, 457 (1927).
[5] *Theory and Applications of Computational Chemistry: The First Forty Years*, edited by C. Dykstra, G. Frenking, K. Kim, and G. Scuseria (Elsevier, Amsterdam, 2005).
[6] R. G. Woolley, Adv. Phys. **25**, 27 (1976).
[7] R. G. Woolley, Mol. Phys. **30**, 649 (1975).
[8] P.-O. Löwdin, Pure Appl. Chem. **61**, 2065 (1989).
[9] R. G. Woolley, J. Mol. Struct.: THEOCHEM **230**, 17 (1991).
[10] R. G. Woolley, J. Math. Chem. **23**, 3 (1998).
[11] B. T. Sutcliffe and R. G. Woolley, Phys. Chem. Chem. Phys. **7**, 3664 (2005).
[12] M. Cafiero and L. Adamowicz, Chem. Phys. Lett. **387**, 136 (2004).
[13] B. T. Sutcliffe and R. G. Woolley, Chem. Phys. Lett. **408**, 445 (2005).
[14] B. T. Sutcliffe, J. Math. Chem. **44**, 988 (2008).
[15] M. Born, Nachr. Akad. Wiss. Goett. II, Math.-Phys. Kl. **6**, 1 (1951).
[16] M. Born and K. Huang, *Dynamical Theory of Crystal Lattices* (Clarendon, Oxford, 1954).
[17] G. Czakó, E. Mátyus, and A. G. Császár, J. Phys. Chem. A **113**, 11665 (2009).
[18] J. Demaison, J. E. Boggs, and A. G. Császár, eds., *Equilibrium Molecular Structures: From Spectroscopy to Quantum Chemistry*, edited by J. Demaison, J. E. Boggs, and A. G. Császár (CRC, Boca Raton, 2011).
[19] H. Primas, *Chemistry, Quantum Mechanics and Reductionism: Perspectives in Theoretical Chemistry* (Springer-Verlag, Berlin, 1981).
[20] U. Müller-Herold, J. Chem. Phys. **124**, 014105 (2006).
[21] E. Mátyus, J. Hutter, U. Müller-Herold, and M. Reiher, Phys. Rev. A **83**, 052512 (2011).
[22] H. Primas, Acta Polytech. Scand. **MA 91**, 83 (1998).
[23] M. Berry, Logic, Methodol. Philos. Sci. **9**, 597 (1994).
[24] R. G. Woolley, Isr. J. Chem. **19**, 30 (1980).
[25] W. Kołos and L. Wolniewicz, J. Chem. Phys. **41**, 3674 (1964).
[26] Y. Suzuki and K. Varga, *Stochastic Variational Approach to Quantum-Mechanical Few-Body Problems* (Springer-Verlag, Berlin, 1998).
[27] M. Cafiero, S. Bubin, and L. Adamowicz, Phys. Chem. Chem. Phys. **5**, 1491 (2003).
[28] H. Nakai, Int. J. Quantum Chem. **86**, 511 (2002).
[29] T. Iordanov and S. Hammes-Schiffer, J. Chem. Phys. **118**, 9489 (2003).
[30] A. Chakraborty, M. V. Pak, and S. Hammes-Schiffer, J. Chem. Phys. **129**, 014101 (2008).
[31] T. Ishimoto, M. Tachikawa, and U. Nagashima, Int. J. Quantum Chem. **109**, 2677 (2009).
[32] A. D. Bochevarov, E. F. Valeev, and C. D. Sherrill, Mol. Phys. **102**, 111 (2004).
[33] M. Stanke, D. Kędziera, S. Bubin, and L. Adamowicz, Phys. Rev. Lett. **99**, 043001 (2007).
[34] S. Hammes-Schiffer and S. R. Billeter, Int. Rev. Phys. Chem. **20**, 591 (2001).
[35] B. T. Sutcliffe, *Coordinate Systems and Transformations, in Handbook of Molecular Physics and Quantum Chemistry*, edited by S. Wilson (Wiley, Chichester, 2003), Vol. 1, pp. 485–500.
[36] B. T. Sutcliffe, *Molecular Hamiltonians, in Handbook of Molecular Physics and Quantum Chemistry*, edited by S. Wilson (Wiley, Chichester, 2003), Vol. 1, pp. 501–525.
[37] R. Paunz, *Spin Eigenfunctions* (Plenum, New York, 1979).
[38] *Explicitly Correlated Wave Functions in Chemistry and Physics*, edited by J. Rychlewski (Kluwer Academic, Dodrecht, 2003).
[39] M. Kamimura, Phys. Rev. A **38**, 621 (1988).
[40] S. A. Alexander, H. J. Monkhorst, and K. Szalewicz, J. Chem. Phys. **85**, 5821 (1986).
[41] S. A. Alexander, H. J. Monkhorst, and K. Szalewicz, J. Chem. Phys. **87**, 3976 (1987).
[42] S. A. Alexander, H. J. Monkhorst, and K. Szalewicz, J. Chem. Phys. **89**, 355 (1988).
[43] I. Mayer, *Simple Theorems, Proofs, and Derivations in Quantum Chemistry* (Kluwer Academic/Plenum, New York, 2003).
[44] P. Claverie and S. Diner, Isr. J. Chem. **19**, 54 (1980).
[45] J. G. R. Tostes, Theor. Chim. Acta **59**, 229 (1981).
[46] S. J. Weininger, J. Chem. Educ. **61**, 939 (1984).
[47] N. Sukumar, Found. Chem. **11**, 7 (2009).
[48] M. Cafiero and L. Adamowicz, Chem. Phys. Lett. **477**, 12 (2009).
[49] M. Cafiero and L. Adamowicz, Int. J. Quantum Chem. **107**, 2679 (2007).
[50] J. Usukura, K. Varga, and Y. Suzuki, Phys. Rev. A **58**, 1918 (1998).
[51] K. Varga, J. Usukura, and Y. Suzuki, Phys. Rev. Lett. **80**, 1876 (1999).
[52] S. Bubin, F. Leonarski, M. Stanke, and L. Adamowicz, J. Chem. Phys. **130**, 124120 (2009).
[53] U. Müller-Herold, Eur. Phys. J. D **49**, 311 (2008).
[54] J. M. Feagin and J. S. Briggs, Phys. Rev. Lett. **57**, 984 (1986).
[55] J. M. Feagin and J. S. Briggs, Phys. Rev. A **37**, 4599 (1988).
[56] J. M. Rost, J. S. Briggs, and J. M. Feagin, Phys. Rev. Lett. **66**, 1642 (1991).
[57] X.-G. Wang and T. Carrington, J. Chem. Phys. **134**, 044313 (2011).
[58] See http://physics.nist.gov/cuu/Constants for CODATA 2006.
[59] A. M. Frolov and V. H. Smith, Phys. Rev. A **49**, 3580 (1994).
[60] Y. K. Ho, Phys. Rev. A **48**, 4780 (1993).
[61] J. P. Karr and L. Hilico, J. Phys. B: **39**, 2095 (2006).
[62] S. Bubin and L. Adamowicz, Phys. Rev. A **74**, 052502 (2006).
[63] S. Bubin, F. Leonarski, M. Stanke, and L. Adamowicz, Chem. Phys. Lett. **477**, 12 (2009).
[64] A. Pérez and O. A. von Lilienfeld, J. Chem. Theory Comput. **7**, 2358 (2011).
[65] A. Fröman and J. L. Kinsey, Phys. Rev. **123**, 2077 (1961).
[66] Z. Chen and C. D. Lin, Phys. Rev. A **42**, 18 (1990).
[67] C. D. Lin, Phys. Rep. **257**, 1 (1995).
[68] P. Pfeifer, "Chiral Molecules: A Superselection Rule Induced by the Radiation Field," Ph.D. dissertation, ETH Zürich, Nr. 6551, ok Gotthard S + D AG, Zürich, 1980.
[69] E. B. Davies, Ann. Inst. Henri Poincaré A **35**, 149 (1981).
[70] P. Claverie and G. Jona-Lasinio, Phys. Rev. A **33**, 2245 (1986).
[71] D. A. McQuarrie, *Statistical Mechanics* (University Science Books, Sausalito, California, 2000).
[72] P. J. E. Peebles, *The Large-Scale Structure of the Universe* (Princeton University, Princeton, NJ, 1980).
[73] R. G. Woolley, Chem. Phys. Lett. **125**, 200 (1986).
[74] H. Primas and U. Müller-Herold, *Quantum-Mechanical System Theory: A Unifying Framework for Observations and Stochastic Processes in Quantum Mechanics*, Advances in Chemical Physics Vol. 38 (Wiley, New York, 1978), pp. 1–107.